Pirfenidone attenuates lung fibrotic fibroblast-mediated fibrotic responses to transforming growth factor-β1

Jin Jin[1,2,6], Shinsaku Togo[1,2], Kotaro Kadoya[1,2], Miniwan Tulafu[1,2], Yukiko Namba[1,2,3], Moe Iwai[1,2], Junko Watanabe[1,2], Kumi Nagahama[1,2], Takahiro Okabe[1,2], Moulid Hidayat[1,2], Yuzo Kodama[1,2], Hideya Kitamura[3], Takashi Ogura[3], Norikazu Kitamura[4], Kazuho Ikeo[4,5], Shinichi Sasaki[7], Shigeru Tominaga[7],and Kazuhisa Takahashi[1,2]

[1]Division of Respiratory Medicine, Juntendo University Faculty of Medicine & Graduate School of Medicine, 2-1-1 Hongo, Bunkyo-ku, Tokyo 113-8421, Japan

[2]Research Institute for Diseases of Old Ages, Juntendo University Graduate School of Medicine, 2-1 -1 Hongo, Bunkyo-ku, Tokyo 113-8421, Japan

[3]Department of Respiratory Medicine Kanagawa Cardiovascular and Respiratory Center, 6-16-1 Tomiokahigashi, Kanazawa-ku, Yokohama, Kanagawa 236-0051, Japan

[4]Center for Information Biology, National Institute of Genetics, 1111 Yata, Mishima, Shizuoka 411-8540, Japan

[5]Department of Genetics, SOKENDAI, 1111 Yata, Mishima, Shizuoka 411-8540, Japan

[6]Department of Respiratory and Critical Care Medicine, Beijing Hospital, National Center of Gerontology, Beijing 100730, People's Republic of China

[7]Department of Respiratory Medicine, Juntendo University Urayasu Hospital, Chiba 279-0001, Japan

Corresponding Author:

Shinsaku Togo, MD, PhD

E-mail: shinsaku@juntendo.ac.jp

24 Running title: Pirfenidone reduces lung fibrosis.

25 **Key words:** Pirfenidone, Collagen triple helix repeat containing protein 1, Four-and-a-half

26 LIM domain protein 2, Transforming growth factor-β1, Bone marrow morphogenic protein-4,

27 Lung fibroblast, Lung fibrosis

28

29

30 **Summary statement**

31 Pirfenidone suppressed TGF-β1-mediated fibrotic processes in fibrotic lung fibroblasts by

32 attenuating CTHRC1 expression, suggesting that CTHRC1 may be a novel therapeutic target

33 for treating patients with lung fibrosis.

34

35

Abstract

Pirfenidone, an antifibrotic agent used for treatment of idiopathic pulmonary fibrosis (IPF), functions by inhibiting myofibroblast differentiation, which is involved in transforming growth factor (TGF)-β1-induced IPF pathogenesis. However, unlike normal lung fibroblasts, the relationship between pirfenidone responses of TGF-β1-induced human fibrotic lung fibroblasts and lung fibrosis is unknown. Here, we investigated the effect of pirfenidone on the functions of two new targets, collagen triple helix repeat containing protein 1 (CTHRC1) and four-and-a-half LIM domain protein 2 (FHL2), which included fibroblast activity, collagen gel contraction, and migration toward fibronectin. Compared to control lung fibroblasts, pirfenidone restored TGF-β1-stimulated fibroblast-mediated collagen gel contraction, migration, and CTHRC1 release in lung fibrotic fibroblasts. Furthermore, pirfenidone attenuated TGF-β1- and CTHRC1-induced fibroblast activity, bone morphogenic protein-4/Gremlin1 upregulation, and α-smooth muscle actin, fibronectin, and FHL2 downregulation, similar to that observed post-CTHRC1 inhibition. In contrast, FHL2 inhibition suppressed migration and fibronectin expression but did not downregulate CTHRC1. Overall, pirfenidone suppressed fibrotic fibroblast-mediated fibrotic processes via inverse regulation of CTHRC1-induced lung fibroblast activity. Thus, CTHRC1 can be used for predicting pirfenidone response and developing new therapeutic target for lung fibrosis.

Introduction

Accumulation of activated lung myofibroblasts and excessive deposition of extracellular matrix (ECM) produced by these cells result in lung tissue contraction, as has been observed in fibrotic lung tissues (Upagupta et al., 2018). This can disrupt lung function, and therefore, inhibition of fibrotic processes may alter the progression of lung fibrosis-related diseases. Diverse mediators, including Krebs von den Lungen (KL)-6 and surfactant protein (SP)-D released from damaged epithelial cells, and inflammatory cytokines (Aono et al., 2012;Xu et al., 2013) and pro-fibrotic growth factors (e.g., transforming growth factor [TGF]-β1 and platelet-derived growth factor [PDGF]) secreted by infiltrated inflammatory cells under conditions of airway inflammation induce fibrosis via autocrine mechanisms involving local lung fibroblast activation in the interstitial alveolar septa (Yoshida et al., 1992;Wynn, 2008).

TGF-β1, a key mediator of normal tissue repair (Blobe et al., 2000), strongly stimulates mesenchymal cells to produce large amounts of ECM, including fibronectin and collagen, resulting in the development of fibrosis (Yoshida et al., 1992). In addition, TGF-β1 stimulates fibroblast chemotaxis toward fibronectin (Sugiura et al., 2006;Togo et al., 2008) and augments fibroblast-mediated contraction of ECM by stimulating contractile stress fibers (α-smooth muscle actin [α-SMA]) (Kobayashi et al., 2006), generating lung fibroblasts that can be used as *in vitro* model of lung fibrosis. Fibronectin released from lung fibroblasts is a known autocrine or paracrine mediator of lung fibroblast-dependent chemotaxis and collagen gel contraction (Kamio et al., 2007;Togo et al., 2008).

Previous reports have shown that corticosteroid treatment does not improve prognosis in patients with idiopathic pulmonary fibrosis (IPF) (Nagai et al., 1999), suggesting that antifibrotic agents may be more useful than anti-inflammatory agents for the treatment of IPF.

Pirfenidone (5-methyl-1-phenyl-2-(1H)-pyridone) is a potent antifibrotic agent that can inhibit the progression of fibrosis in patients with IPF. Pirfenidone attenuates the expression of procollagen, TGF-β1, and PDGF at the transcriptional level and ameliorates bleomycin-induced lung fibrosis in a rodent model (Iyer et al., 1999a; Iyer et al., 1999b;Gurujeyalakshmi et al., 1999). However, the precise mechanisms via which pirfenidone suppresses lung fibrosis are still unclear.

In this study, we evaluated the effects pirfenidone on TGF-β1-mediated contraction of ECM and migration toward fibronectin of lung fibroblasts isolated from patients with lung fibrosis and compared them with those of normal lung fibroblasts for understanding the mechanisms mediating lung fibroblast-dependent antifibrotic effects of pirfenidone. In addition, we focused on the two molecular targets of pirfenidone, namely, collagen triple helix repeat containing protein 1 (CTHRC1) and four-and-a-half LIM domain protein 2 (FHL2); the levels of these two proteins were previously demonstrated to be attenuated in the bleomycin-induced lung fibrosis model and CTHRC1 secretion was inhibited in the TGF-β1–induced normal primary human lung fibroblasts (Bauer er al.,2015). Our results provided important insights into pirfenidone-mediated antifibrotic processes. Furthermore, we established novel evidence of clinical markers for predicting responses to pirfenidone, which will assist in selecting therapy based on *in vitro* functional measurements of lung fibrotic fibroblast and clinicopathological information formally evaluated using multidisciplinary diagnosis (MDD).

Results

Clinical and demographic characteristics

The clinical and demographic characteristics of the patients are shown in Table 1. The two

103 groups were similar in terms of age, smoking status, and sex. However, they differed
104 significantly in lung function; as expected, patients with lung fibrosis had a lower percent
105 forced vital capacity (% FVC). Histological examination revealed that of 12 patients with lung
106 fibrosis not receiving medication, six had nonspecific interstitial pneumonia (NSIP), and six
107 had usual interstitial pneumonia (UIP). Clinical diagnoses revealed three patients with IPF,
108 five patients with NSIP, and four patients with chronic hypersensitivity pneumonitis (CHP).

109 Table 1. Clinical and demographic characteristics of the patients

	No. of control patients	Mean ± SD	No. of IP patients	Mean ± SD	*P* value
Age, years	12	64.5 ± 8.1	12	59.1 ± 14.7	0.28
Sex, no. male/female	9/3		8/4		1.00
Smoking history (yes/no)					
	8/4		8/4		1.00
Pack-years	8	712.5 ± 374.4	8	537.5 ± 498.2	0.44
% FVC	12	99.2 ± 4.1	12	85.2 ± 4.8	0.04
KL-6	12	None	12	1422.3 ± 595.0	
SP-D	12	None	12	200.7 ± 77.8	
Clinical diagnosis	12	None	3 IPF, 5 NSIP, 4 CHP*		
Histological pattern	12	None	6 UIP, 6 NSIP*		

110 Abbreviations: CHP, chronic hypersensitivity pneumonitis; FVC, forced vital capacity; KL: Krebs von den Lungen; SP: surfactant
111 protein; IP: interstitial pneumonia; IPF, idiopathic pulmonary fibrosis; NSIP, nonspecific interstitial pneumonia; UIP, usual
112 interstitial pneumonia. *, Diagnosed by multidisciplinary diagnosis (MDD).

113 **Effects of pirfenidone on TGF-β1-stimulated fibroblast activity**

114 Pirfenidone inhibited collagen gel contraction of human fetal lung fibroblast-1 (HFL-1) in a
115 concentration-dependent manner, but did not affect chemotaxis when added alone to HFL-1
116 cells (Fig. 1A, C).

Next, we investigated whether pirfenidone altered the TGF-β1-induced increase in collagen gel contraction and chemotaxis towards fibronectin in HFL-1 cells. Pirfenidone treatment reduced TGF-β1-induced collagen gel contraction and chemotaxis in HFL-1 cells in a concentration-dependent manner ($P < 0.05$ for 100 μg/mL pirfenidone ± 10 pM TGF-β1 versus control; Fig. 1A, C). Pirfenidone abolished HFL-1-mediated gel contraction and chemotaxis in the presence of less than 10 pM TGF-β1 ($P < 0.05$). However, in the presence of 100 pM TGF-β1, pirfenidone did not inhibit HFL-1-mediated gel contraction and chemotaxis (Fig. 1B, D).

Although the maximum plasma concentration (C_{max}) of pirfenidone, which is typically used for treating patients with IPF at dosage up to 1800 mg/day, is 15.7 μg/mL after administration of 801 mg pirfenidone (Rubino et al., 2009), higher concentrations may be used; indeed, pirfenidone is widely used at concentrations above 100 μg/mL *in vitro* in the laboratory setting (Conte et al., 2014). Therefore, we used 100 μg/mL pirfenidone, with or without 10 pM TGF-β1, in our subsequent experiments on adult human primary lung fibroblasts.

Notably, gel contraction and chemotaxis were attenuated in cells treated with 100 μg/mL pirfenidone alone or in combination with 10 pM TGF-β1 (Fig. 2A, C). This inhibitory effect was higher in fibroblasts from fibrotic lungs than in control fibroblasts (gel contraction: $P < 0.001$ and 0.05, chemotaxis: $P < 0.05$ and $P = 0.16$, fibrotic vs. normal lung; Fig. 2B, D). However, there were no differences in the effects of fibrotic lung fibroblasts from patients with UIP compared to those from patients with NSIP. At the end of the incubation, cell numbers or viability in the gels in pirfenidone- and/or TGF-β1-treated groups were not different from those in the control group, as assessed by 3-(4,5-dimethylthiazol-2-yl)-2,5-diphenyltetrazolium

bromide (MTT) assays (data not shown).

High sensitivity of TGF-β1-induced fibrotic mediators in fibrotic lung fibroblasts

CTHRC1 is a marker of activated stromal cells (Duarte et al., 2014). As pirfenidone suppresses both TGF-β1-induced CTHRC1 and FHL2 (Bauer et al., 2015), we assessed TGF-β1-induced changes in cytoplasmic CTHRC1 and FHL2 expression levels in fibrotic fibroblasts using immunoblotting. The relative increases in CTHRC1 and FHL2 upon TGF-β1 stimulation were higher in fibrotic fibroblasts than in control fibroblasts; however, there were no differences in fibrotic lung fibroblasts between patients with UIP and those with NSIP (CTHRC1: control, $P = 0.109$ versus lung fibrosis, $P = 0.003$; FHL2: control, $P = 0.360$ versus lung fibrosis, $P = 0.006$; Fig. 3A, B). Since CTHRC1 is a secreted protein and a previous report showed that CTHRC1 was present in plasma of individual patients (Duarte et al., 2014); therefore, we also measured release of CTHRC1 protein from human lung fibroblasts using enzyme-linked immunosorbent assay (ELISA). The relative increases in CTHRC1 releasing from fibroblasts upon TGF-β1 stimulation were higher from fibrotic fibroblasts than from control fibroblasts. The fold increase in CTHRC1 in the presence of TGF-β1 stimulation (1.347 ± 0.246 in control fibroblasts versus 3.610 ± 0.662 in fibrotic fibroblasts; $P = 0.004$) was higher in fibroblasts from fibrotic lungs than in control fibroblasts. The suppressive effects of pirfenidone on CTHRC1 release from TGF-β1-induced fibroblasts was higher in fibrotic lung fibroblasts than in control fibroblasts (control: $P = 0.111$; IP: $P < 0.001$); in contrast, the suppressive effects of pirfenidone alone were similar with respect to release of CTHRC1 (control: $P = 0.004$; IP: $P = 0.001$). The fold reduction in CTHRC1 in the presence of pirfenidone following TGF-β1 stimulation (0.139 ± 0.069 in control fibroblasts versus 0.400 ±

163 0.064 in fibrotic fibroblasts; P = 0.018) was higher in fibroblasts from fibrotic lungs than in
164 control fibroblasts (All folds calculated by difference value after treatment / initial value) (Fig.
165 3C).

166 Fibroblasts are known to release mediators, including TGF-β1 (Sugiura et al., 2006;
167 Togo et al., 2008) and prostaglandin E_2 (PGE_2) (Kohyama et al., 2001; Zhu et al., 2001),
168 which can modulate chemotaxis and collagen gel contraction in an autocrine or paracrine
169 manner. To determine whether these mediators directly contribute to the suppression of
170 collagen gel contraction and chemotaxis induced by pirfenidone, the release of these
171 mediators into the monolayer culture medium was evaluated using ELISA. Notably,
172 pirfenidone did not affect TGF-β1 levels in culture medium of control and fibrotic fibroblasts
173 (Fig. 3D). Furthermore, the ability of pirfenidone to modulate PGE_2 release and inducible
174 cyclooxygenase 2 (COX2) expression was further assessed in culture medium from HFL-1
175 cells. Pirfenidone did not stimulate PGE_2 release or COX2 expression with or without TGF-β1
176 in fibroblasts (Fig. S1A, B). These results indicated that the pirfenidone-regulated molecules
177 CTHRC1 and FHL2 may play a dominant role in pirfenidone-mediated fibroblast activity
178 rather than exert direct effects on TGF-β1-mediated autocrine/paracrine regulation in
179 fibroblasts.

180

181 **Effects of pirfenidone on TGF-β1-mediated fibrotic regulators in lung fibroblasts**

182 Next, we assessed whether pirfenidone altered targets related to TGF-β1-mediated fibrotic
183 processes in HFL-1 cells. Treatment with pirfenidone significantly reduced
184 TGF-β1-augmented expression of CTHRC1, FHL2, α-SMA, fibronectin, and Gremlin1
185 ($P < 0.05$; Fig. 4A–E, G) and reversed TGF-β1-dependent suppression of bone morphogenic

186 protein-4 (BMP4; $P < 0.05$; Fig. 4A, F).

187

188 **Effects of pirfenidone on CTHRC1-mediated regulation in lung fibroblasts**

189 We investigated the effects of recombinant human (rh) CTHRC1 on HFL1-mediated collagen
190 gel contraction and chemotaxis. rhCTHRC1 (10–1000 ng/mL) stimulated gel contraction and
191 chemotaxis toward fibronectin in a concentration-dependent manner ($P < 0.05$) compared to
192 the control (Fig. 5A–C), accompanied by concentration-dependent upregulation of FHL2,
193 α-SMA, fibronectin, and Gremlin1 and downregulation of BMP4 (Fig. 5A). According to a
194 previous report on detection of CTHRC1 plasma levels, we used 100 ng/mL rhCTHRC1 with
195 or without 10 pM TGF-β1 in our studies on HFL-1cells (Duarte et al., 2014). Pirfenidone
196 significantly attenuated rhCTHRC1-induced gel contraction and chemotaxis ($P < 0.05$; Fig.
197 5E, F); it also suppressed rhCTHRC1-augmented FHL2, α-SMA, fibronectin, and Gremlin1
198 expression ($P < 0.05$; Fig. 5D–I, K) and reversed rhCTHRC1-dependent suppression of
199 BMP4 ($P < 0.05$; Fig. 5D, J).

200

201 **Inhibition of CTHRC1- and FHL2-mediated regulation of HFL-1**

202 To investigate the functional roles of the pirfenidone-mediated targets CTHRC1 and FHL2 in
203 lung fibroblasts, we knocked down these targets in HFL-1 cells. Silencing of *CTHRC1* led to a
204 complete reversal of targets related to TGF-β1-mediated fibrotic processes, i.e., reduction in
205 FHL2, α-SMA, fibronectin, and Gremlin1 expression and increase in BMP4 expression (Fig.
206 6A). Furthermore, *CTHRC1* knockdown attenuated gel contraction and chemotaxis (Fig. 6B,
207 C). However, silencing of *FHL2* did not affect CTHRC1, α-SMA , BMP4, and Gremlin1
208 expression and gel contraction, but reduced fibronectin expression and chemotaxis (Fig. 6D,

209 E).

210

211 **Effects of pirfenidone on *in vitro* TGF-β1-stimulated fibroblast activity and biomarkers**
212 **of lung fibrosis**

213 Considering our observation that pirfenidone in fibrotic lung fibroblasts enhanced their
214 sensitivity to TGF-β1-induced fibrosis compared to normal fibroblasts, we investigated
215 whether our *in vitro* data was clinically significant. Toward this objective, we measured serum
216 levels of the lung fibrosis biomarkers KL-6 and SP-D in serum of patients with lung fibrosis at
217 the time of primary lung fibroblast sample collection. The ability of pirfenidone to abrogate the
218 TGF-β1-induced increase in collagen gel contraction correlated positively with SP-D levels (r^2
219 = 0.388, *P* = 0.031, Fig. 7B) but not with KL-6 levels (Fig. 7A). In contrast, the inhibitory
220 effects of pirfenidone on TGF-β1-induced migration correlated negatively with KL-6 levels (r^2
221 = 0.380, *P* = 0.033, Fig. 7C) but not with SP-D levels (Fig. 7D). No other clinical or
222 histopathological and spirometric parameters, such as sustainer and rapid decliner
223 categories according to forced vital capacity (FVC) reduction rates, were related to *in vitro*
224 fibroblast response to pirfenidone treatment or to *in vitro* fibroblast activity.

225

226 **DISCUSSION**

227 In this study, we observed that changes in the fibrotic lung fibroblast phenotype resulted in
228 increased response to the pirfenidone-suppressed bioactivity of lung fibroblasts, leading to
229 inhibition of collagen gel contraction and migration, following TGF-β1-mediated activation.
230 Previous reports have shown that pirfenidone reduces proliferation, migration,

fibroblast-embedded collagen gel contraction, ECM production, and TGF-β1-mediated differentiation into myofibroblasts by attenuating the effect of TGF-β1 and its downstream targets, including phosphorylation of Smad3, connective tissue growth factor, p38, and Akt in human fibroblasts (Conte et al., 2014; Hall et al., 2018; Lin et al., 2009;Saito et al., 2012;Shi et al., 2011;;Sun et al., 2018), which support our current results. Pirfenidone prevented changes in the fibrotic fibroblast phenotype, increasing proliferation and migration and enhancing levels of phospho-Smad3, phospho-signal transducer and activator of transcription 3, α-SMA, and collagen in the context of IPF (Epstein Shochet et al., 2018). We clarified the mechanisms via which CTHRC1 and FHL-2 (Bauer et al., 2015} were stimulated by TGF-β1 in lung fibrotic fibroblasts compared to in control fibroblasts. Our results showed that pirfenidone suppressed CTHRC1-induced migration toward to fibronectin, gel contraction, and α-SMA and fibronectin expression and increased the BMP4/Gremlin1 ratio. In additionr, pirfenidone also suppressed FHL-2-mediated fibroblast migration.

CTHRC1 is expressed by activated stromal cells of diverse origin and co-expressed with α-SMA. Elevated CTHRC1 levels were detected in patients with inflammatory conditions, including rheumatoid arthritis, and CTHRC1 is considered a marker of tissue remodeling, inflammation, or wounding (Duarte et al., 2014; Shekhani et al., 2016). A previous report has shown that CTHRC1 plays a protective role in pulmonary fibrosis and tissue repair and may be clinically applied for treating fibrosis as it decreases collagen matrix deposition by inhibiting Smad2/3 activation (LeClair and Lindner, 2007). In addition, rhCTHRC1 inhibits TGF-β1-stimulated collagen type I synthesis and promotes skin repair in keloid fibroblasts (Li et al., 2011; Pyagay et al., 2005). The systemic loss of CTHRC1 increased TGF-β1-mediated excess matrix deposition and induced the development of bleomycin-induced lung fibrosis in

mice (Binks et al., 2017). Furthermore, TGF-β1 and BMP-4, which belong to the TGF-β superfamily of ligands, stimulate CTHRC1 expression, and overexpression of CTHRC1 in smooth muscle cells, and embryonic fibroblasts treated with exogenous rhCTHRC1 increases migration (Pyagay et al., 2005; Shekhani et al., 2016). In this study, we demonstrated that fibrotic fibroblasts showed altered phenotypes of TGF-β1-stimulated CTHRC1 expression and pirfenidone-dependent suppression of CTHRC1 expression after TGF-β1 treatment. In addition, rhCTHRC1 stimulated lung fibroblast-mediated gel contraction and migration, and *CTHRC1* knockdown suppressed fibronectin expression, migration toward fibronectin, and gel contraction. Pirfenidone restored TGF-β1- and rhCTHRC1-dependent suppression of BMP4 expression, which was previously reported to reduce lung fibroblast proliferation and TGF-β1-induced synthesis of ECM components, including fibronectin (Jeffery et al., 2005; Pegorier et al., 2010). In the present study, pirfenidone also reduced the levels of the BMP4 antagonist Gremlin1, which was previously implicated in the development of lung fibrosis (Myllarniemi et al., 2008), when stimulated by TGF-β1 and rhCTHRC1. These results indicated that CTHRC1 acted as a costimulator of TGF-β1-mediated fibrotic processes in fibrotic fibroblasts rather than as a suppresser of fibrosis. Thus, CTHRC1 could be a dominant target for pirfenidone-mediated antifibrotic mechanisms in fibrotic lung fibroblasts.

FHL2 participates in tissue wound healing and is associated with fibrogenesis (Gullotti et al., 2011; Wixler et al., 2007). *Fhl2* $^{-/-}$ mice develop hepatic fibrogenesis (Dahan et al., 2017), and *Fhl2*-deficient embryonic fibroblasts show reduced collagen contraction and cell migration, resulting in impaired wound healing (Wixler et al., 2007). However, in contrast to CTHRC1, FHL2 has been reported to positively regulate the expression of collagen types I

277 and III in an FHL2-induced BLM-treated lung fibrosis model; this process tended to involve
278 acceleration of lung inflammation rather than direct FHL2-induced fibrotic mechanisms
279 (Alnajar et al., 2013; Kirfel et al., 2008; Park et al., 2008). Furthermore, FHL2 induces α-SMA
280 (Wixler et al., 2007) and is stimulated by TGF-β1 (Bauer et al., 2015; Muller et al., 2002}. In
281 this study, we also demonstrated that FHL2 was further stimulated by TGF-β1 in fibrotic
282 fibroblasts compared to control fibroblasts and that pirfenidone suppressed
283 TGF-β1-stimulated FHL2 expression. However, *FHL2* knockdown suppressed only
284 fibronectin expression and migration toward fibronectin, but did not affect gel contraction,
285 other TGF-β1-mediated fibroblast regulators, or CTHRC1 expression. As *CTHRC1*
286 knockdown attenuated FHL2 expression, FHL2 may play a role in lung fibroblast-mediated
287 fibrosis following TGF-β1-induced upregulation of *CTHRC1* (Fig. 7E).

288 Clinically, patients with IPF who showed predicted vital capacity (VC) of more than
289 70% and lowest oxygen satuation in blood during 6 min walking tests (less than 90% at
290 baseline) are most likely to benefit from pirfenidone therapy (Azuma et al., 2011). The
291 expression levels of pirfenidone-targeted translational gene markers (*GREM1*, *CTHRC1*, and
292 *FHL2*) showed significant negative correlation with the percentage diffusing capacity of
293 carbon monoxide (%DLCO), and was associated with IPF disease severity (Bauer et al.,
294 2015). However, little is known regarding the surrogate markers of pirfenidone response. In
295 this study, we demonstrated that the magnitude of pirfenidone-dependent suppression of
296 TGF-β1-induced gel contraction and migration was positively related to serum SP-D levels
297 and negatively related to serum KL-6 levels, but was not related to any other clinical
298 parameters, including histological pattern and lung function (%VC, %FVC, and %DLCO).
299 These diverse phenotypic responses to pirfenidone in fibrotic lung fibroblasts and our *in vitro*

results related to serum biomarkers suggested that the progressive state of lung fibrosis with increasing SP-D/KL-6 ratios may be associated with better clinical outcomes (Fig. 7E). This analysis described the relative usefulness of other clinical parameters at baseline when estimating the predictable surrogate marker of patients with lung fibrosis as candidates for pirfenidone therapy.

The results presented here provided evidence regarding the high sensitivity of fibrotic fibroblasts to pirfenidone, which mediated TGF-β1-induced fibrotic processes. However, our study has certain limitations. For example, we used limited number of patients' fibroblasts lines and did not assess plasma levels of CTHRC1 as a clinical surrogate marker for predicting pirfenidone response. Instead, we performed functional experiments in lung fibroblasts and analyzed the responses of human lung fibrosis patient-derived lung fibroblast samples to pirfenidone for determining the utility of CTHRC1 as a potential therapeutic target and for predicting pirfenidone responses in lung fibroblast-mediated fibrosis regulation. Our observations provide preliminary evidence regarding identification of pirfenidone responses in personalized therapies and the application of CTHRC1 as a novel biomarker with translational value for predicting pirfenidone responses in patients with lung fibrosis.

MATERIALS AND METHOD

Materials

Cell culture medium (Dulbecco's modified Eagle's medium [DMEM]) was purchased from Wako (Osaka, Japan). Fetal calf serum was purchased from Sigma-Aldrich (St. Louis, MO, USA). TGF-β1 was obtained from R & D Systems (Minneapolis, MN, USA), and rhCTHRC1

322 was from Abcam (Cambridge, UK). Pirfenidone was provided by Shionogi & Co. Ltd. (Osaka,
323 Japan) and was dissolved in 100% dimethylsulfoxide (DMSO). The amount of DMSO added
324 did not affect the results of the bioassays (Hatzelmann and Schudt, 2001). Preliminary
325 experiments with MTT demonstrated that the concentrations of pirfenidone and DMSO used
326 in this study did not show any significant cytotoxicity in fibroblasts (data not shown).
327
328 **Cell culture**
329 HFL-1 cells were obtained from the American Type Culture Collection (CCL-153; Manassas,
330 VA, USA). Primary lung fibroblasts were obtained from 12 patients with lung fibrosis, as
331 diagnosed by a multidisciplinary team using the gold standard approach (Chung and Lynch,
332 2016), and 12 patients without clinical airway symptom or lung functional abnormalities as a
333 control group (Table 1). The Institutional Review Board of Juntendo University School of
334 Medicine and Kanagawa Cardiovascular and Respiratory Center approved the procedures.
335 All patients provided written, informed consent (approval no. 2012173). Human primary lung
336 parenchymal fibroblasts from patients undergoing lung resection were cultured as described
337 previously (Holz et al., 2004). Tissues were obtained from areas of macroscopically normal
338 lung parenchyma, distal to any tumor masses, in the control fibroblast group. Cells were
339 collected from areas of complete fibrosis (resembling a honey comb), avoiding large airways,
340 vessels and pleural surface in the lung fibrosis fibroblast group. These cells were cultured as
341 described above. Cells from the outgrowths of these cells, termed “P0,” were frozen for later
342 use; these cells displayed typical fibroblast morphology and were confirmed to be positive for
343 vimentin and negative for cytokeratin. For chemotaxis, three-dimensional collagen gel
344 contraction, and ELISA analyses, primary lung fibroblasts were used at passages 4–6 after

345 isolation to exclude the effects of differences in passage number and culturing conditions.

346

347 **Fibroblast chemotaxis**

348 HFL-1 cell chemotaxis was assessed using the Boyden blindwell chamber technique
349 (Neuroprobe, Inc., Gaithersburg, MD, USA) as previously described (Boyden, 1962). In
350 experiments with TGF-β1 or rhCTHRC1, pirfenidone was added to the wells of the upper
351 chamber, whereas human fibronectin (20 µg/mL) was placed in the bottom chamber as the
352 chemoattractant. The two wells were separated by an 8-µM pore filter (Nucleopore,
353 Pleasanton, CA, USA). The chambers were incubated at 37°C in a humid atmosphere
354 containing 5% CO_2 for 8 h, after which the cells on top of the filter were removed by scraping.
355 The cells that had migrated through the filter were then fixed, stained with DiffQuick Sysmex
356 (16920), and mounted on glass microscope slides. Migration was assessed by counting the
357 number of cells in five high-power fields. Replica experiments were performed in triplicate,
358 and replicates with separate cell cultures were performed on separate occasions. Wells with
359 serum-free DMEM were used as negative controls.

360

361 **Collagen gel contraction assay**

362 Type I collagen (rat tail tendon collagen) was extracted from rat tail tendons as previously
363 described (Elsdale and Bard, 1972). The effects of pirfenidone on fibroblast-mediated gel
364 contraction were determined in the presence or absence of TGF-β1 or rhCTHRC1 using a
365 modification of the method developed by Bell et al. (Bell et al., 1979). The floating gels were
366 cultured for up to 3 days, and the ability of the fibroblasts to contact the gels was determined
367 by quantifying the area of the gels daily using an LAS4000 image analyzer (GE Healthcare

Bio-Science AB, Uppsala, Sweden). Data are expressed as the gel area percentage compared to the original gel size.

Measurement of CTHRC1, TGF-β1, and PGE_2 levels

Cultures were maintained for 48 h to quantify CTHRC1, TGF-β1, and PGE_2 levels. After 48 h, media were collected, frozen, and stored at -80°C until analysis. CTHRC1, TGF-β_1, and PGE_2 production by the cells was determined using human CTHRC1 (LifeSpan BioScienceds, Inc., Seattle, WA, USA), TGF-β_1 (R&D Systems), and PGE_2 immunoassays (Cayman Chemical, Ann Harbor, MI, USA), respectively, according to the manufacturers' instructions.

Western blot analysis

To standardize culture conditions, cells were passaged at a density of 5×10^4 cells/mL, cultured for 48 h, and then collected for preparation of whole cell lysates. The medium was changed to DMEM without serum for 24 h, followed by treatment with TGF-β1 (10 pM) or rhCTHRC1 (100 ng/mL) in the presence or absence of pirfenidone (100 μg/mL) for 48 h or with various concentrations of rhCTHRC1 for 8 h. Primary antibodies against the following proteins were used for western blotting: CTHRC1 (1:5000 dilution; Proteintech, Rosemont, IL, USA; cat. no. 16534-1-AP), FHL2 (1:1000 dilution; Abcam, Cambridge, UK; cat. no. ab66399), α-SMA (1:1000 dilution; Sigma-Aldrich; cat. no. A2547), fibronectin (1:1000 dilution; Enzo Life Sciences, Inc., Farmingdale, NY, USA; cat. no. BML-FG6010-0100), BMP-4 (1:1000 dilution; Abcam; cat. no. ab39973), Gremlin1 (1:1000 dilution; Thermo Fisher Scientific, Waltham, MA, USA; cat. no. PA5-13123), β-actin (1:5000 dilution; Wako Pure Chemical Industries; cat. no. 013-24553), and COX2 (1:1000 dilution; Abcam; cat. no. ab169782). Bound antibodies were

visualized using peroxidase-conjugated secondary antibodies and enhanced chemiluminescence with a LAS4000 image analyzer (GE Healthcare Bio-Science AB), and band intensity was analyzed Image Gauge software (LAS-400 Plus; Fujifilm).

Small interfering RNA (siRNA)-mediated knockdown assays

Commercial siRNA targeting CTHRC1 (10620318; Life Technologies, Carlsbad, CA, USA) and FHL2 (1027416; Qiagen, Valencia, CA, USA) was transfected using RNAiMAX transfection reagent (13778-150; Life Technologies) diluted in Opti-MEM (31985062; Gibco/Life Technologies) according to the manufacturers' instructions. HLF-1 cells were plated at 1×10^5 cells/mL and incubated for 24 h, and were used for transfection when they reached 50–70% confluency. Predetermined concentrations of siRNA were used to achieve more than 70% knockdown. To suppress endogenous CTHRC1 and FHL2 in fibroblasts, the cells were transfected for 24 h with 50 nM CTHRC1 siRNA or 15 nM FHL2 siRNA. A scrambled siRNA probe was used as a control. After silencing CTHRC1 or FHL2 with siRNA, the cells were analyzed using western blotting, and collagen gel contraction assays and chemotaxis experiments were performed.

Statistical analysis

Results are expressed as means ± standard errors of the means (SEMs). We used Student's t tests to determine differences between groups and linear regression to relationship. For experiments in which paired samples within a group were available, we used paired Student's t tests. For these comparisons, each patient was considered an individual data point.

Differences with *P* values less than 0.05 were considered significant. Data were analyzed using Prism 6 software (GraphPad Inc., San Diego, CA, USA).

Acknowledgments

We thank X. Liu, F. Sakai, T. Takemura, T. Iwasawa, I. Taki, L. Ning, N. Okamoto, T. Ito, R. Mineki, F. Takahashi, and E. Kobayashi for technical assistance and advice. We thank T. Takeda and N. Kondo for providing us CAGE result to clarified mechanism from RIKEN Center for Life Science Technologies. We thank Tadayuki Takeda and Naoto Kondo for providing us CAGE result try to further clarify present mechanism from RIKEN Center for Life Science Technologies. We thank S. Kusano and A. Kusano for drawing figure 7E design from KUSANO DESIGN OFFICE (Tokyo, Japan). And we acknowledges the International Fellowship Program, Takeda Science Foundation.

Competing interests

The authors declare no competing or financial interests.

Funding

This study was partially supported by the Platform Project for Supporting Drug Discovery and Life Science Research from AMED (grant no. JP16am0101057).

Abbreviation list:

433 α-SMA: α-smooth muscle actin

434 BMP-4: bone morphogenetic protein-4

435 CHP: chronic hypersensitivity pneumonitis

436 COX2: cyclooxygenase 2

437 CTHRC1: collagen triple helix repeat containing protein 1

438 %DLCO: percent diffusing capacity of carbon monoxide

439 ECM: extracellular matrix

440 ELISA: enzyme-linked immuno sorbent assay

441 FHL2: four-and-a-half LIM domain protein 2

442 %FVC: percent forced vital capacity

443 HFL-1: human fetal lung fibroblast-1

444 IP: interstitial pneumonia

445 IPF: idiopathic pulmonary fibrosis

446 KL: Krebs von den Lungen

447 MDD: multidisciplinary diagnosis

448 NSIP: nonspecific interstitial pneumonia

449 PDGF: platelet-derived growth factor

450 PGE2: prostaglandin E2

451 Rh: recombinant human

452 SEM: standard errors of the means

453 SP: surfactant protein

454 TGF: transforming growth factor

455 UIP: usual interstitial pneumonia

456 VC: vital capacity

457

458 **References**

459 **Alnajar, A., Nordhoff, C., Schied, T., Chiquet-Ehrismann, R., Loser, K., Vogl, T.,**
460 **Ludwig, S. and Wixler, V.** (2013). The LIM-only protein FHL2 attenuates lung inflammation
461 during bleomycin-induced fibrosis. *PLoS One* **8**, e81356.
462 **Aono, Y., Ledford, J. G., Mukherjee, S., Ogawa, H., Nishioka, Y., Sone, S., Beers,**
463 **M. F., Noble, P. W. and Wright, J. R.** (2012). Surfactant protein-D regulates effector cell
464 function and fibrotic lung remodeling in response to bleomycin injury. *Am J Respir Crit Care*
465 *Med* **185**, 525-36.
466 **Azuma, A., Taguchi, Y., Ogura, T., Ebina, M., Taniguchi, H., Kondoh, Y., Suga, M.,**
467 **Takahashi, H., Nakata, K., Sato, A. et al.** (2011). Exploratory analysis of a phase III trial of
468 pirfenidone identifies a subpopulation of patients with idiopathic pulmonary fibrosis as
469 benefiting from treatment. *Respir Res* **12**, 143.
470 **Bauer, Y., Tedrow, J., de Bernard, S., Birker-Robaczewska, M., Gibson, K. F.,**
471 **Guardela, B. J., Hess, P., Klenk, A., Lindell, K. O., Poirey, S. et al.** (2015). A novel genomic

472 signature with translational significance for human idiopathic pulmonary fibrosis. *Am J Respir*
473 *Cell Mol Biol* **52**, 217-31.
474 **Bell, E., Ivarsson, B. and Merrill, C.** (1979). Production of a tissue-like structure by
475 contraction of collagen lattices by human fibroblasts of different proliferative potential in vitro.
476 *Proc Natl Acad Sci U S A* **76**, 1274-8.
477 **Binks, A. P., Beyer, M., Miller, R. and LeClair, R. J.** (2017). Cthrc1 lowers
478 pulmonary collagen associated with bleomycin-induced fibrosis and protects lung function.
479 *Physiol Rep* **5**.
480 **Blobe, G. C., Schiemann, W. P. and Lodish, H. F.** (2000). Role of transforming
481 growth factor beta in human disease. *N Engl J Med* **342**, 1350-8.
482 **Boyden, S.** (1962). The chemotactic effect of mixtures of antibody and antigen on
483 polymorphonuclear leucocytes. *J Exp Med* **115**, 453-66.
484 **Chung, J. H. and Lynch, D. A.** (2016). The Value of a Multidisciplinary Approach to
485 the Diagnosis of Usual Interstitial Pneumonitis and Idiopathic Pulmonary Fibrosis: Radiology,
486 Pathology, and Clinical Correlation. *AJR Am J Roentgenol* **206**, 463-71.
487 **Conte, E., Gili, E., Fagone, E., Fruciano, M., Iemmolo, M. and Vancheri, C.**
488 (2014). Effect of pirfenidone on proliferation, TGF-beta-induced myofibroblast differentiation
489 and fibrogenic activity of primary human lung fibroblasts. *Eur J Pharm Sci* **58**, 13-9.
490 **Dahan, J., Levillayer, F., Xia, T., Nouet, Y., Werts, C., Fanton d'Andon, M.,**
491 **Adib-Conquy, M., Cassard-Doulcier, A. M., Khanna, V., Chen, J. et al.** (2017). LIM-Only
492 Protein FHL2 Is a Negative Regulator of Transforming Growth Factor beta1 Expression. *Mol*
493 *Cell Biol* **37**.
494 **Duarte, C. W., Stohn, J. P., Wang, Q., Emery, I. F., Prueser, A. and Lindner, V.**
495 (2014). Elevated plasma levels of the pituitary hormone Cthrc1 in individuals with red hair but
496 not in patients with solid tumors. *PLoS One* **9**, e100449.
497 **Elsdale, T. and Bard, J.** (1972). Collagen substrata for studies on cell behavior. *J*
498 *Cell Biol* **54**, 626-37.
499 **Epstein Shochet, G., Wollin, L. and Shitrit, D.** (2018). Fibroblast-matrix interplay:
500 Nintedanib and pirfenidone modulate the effect of IPF fibroblast-conditioned matrix on normal
501 fibroblast phenotype. *Respirology* **23**, 756-763.
502 **Gullotti, L., Czerwitzki, J., Kirfel, J., Propping, P., Rahner, N., Steinke, V., Kahl,**
503 **P., Engel, C., Schule, R., Buettner, R. et al.** (2011). FHL2 expression in peritumoural
504 fibroblasts correlates with lymphatic metastasis in sporadic but not in HNPCC-associated
505 colon cancer. *Lab Invest* **91**, 1695-705.
506 **Gurujeyalakshmi, G., Hollinger, M. A. and Giri, S. N.** (1999). Pirfenidone inhibits

PDGF isoforms in bleomycin hamster model of lung fibrosis at the translational level. *Am J Physiol* **276**, L311-8.

Hall, C. L., Wells, A. R. and Leung, K. P. (2018). Pirfenidone reduces profibrotic responses in human dermal myofibroblasts, in vitro. *Lab Invest* **98**, 640-655.

Hatzelmann, A. and Schudt, C. (2001). Anti-inflammatory and immunomodulatory potential of the novel PDE4 inhibitor roflumilast in vitro. *J Pharmacol Exp Ther* **297**, 267-79.

Holz, O., Zuhlke, I., Jaksztat, E., Muller, K. C., Welker, L., Nakashima, M., Diemel, K. D., Branscheid, D., Magnussen, H. and Jorres, R. A. (2004). Lung fibroblasts from patients with emphysema show a reduced proliferation rate in culture. *Eur Respir J* **24**, 575-9.

Iyer, S. N., Gurujeyalakshmi, G. and Giri, S. N. (1999a). Effects of pirfenidone on procollagen gene expression at the transcriptional level in bleomycin hamster model of lung fibrosis. *J Pharmacol Exp Ther* **289**, 211-8.

Iyer, S. N., Gurujeyalakshmi, G. and Giri, S. N. (1999b). Effects of pirfenidone on transforming growth factor-beta gene expression at the transcriptional level in bleomycin hamster model of lung fibrosis. *J Pharmacol Exp Ther* **291**, 367-73.

Jeffery, T. K., Upton, P. D., Trembath, R. C. and Morrell, N. W. (2005). BMP4 inhibits proliferation and promotes myocyte differentiation of lung fibroblasts via Smad1 and JNK pathways. *Am J Physiol Lung Cell Mol Physiol* **288**, L370-8.

Kamio, K., Liu, X., Sugiura, H., Togo, S., Kobayashi, T., Kawasaki, S., Wang, X., Mao, L., Ahn, Y., Hogaboam, C. et al. (2007). Prostacyclin analogs inhibit fibroblast contraction of collagen gels through the cAMP-PKA pathway. *Am J Respir Cell Mol Biol* **37**, 113-20.

Kirfel, J., Pantelis, D., Kabba, M., Kahl, P., Roper, A., Kalff, J. C. and Buettner, R. (2008). Impaired intestinal wound healing in Fhl2-deficient mice is due to disturbed collagen metabolism. *Exp Cell Res* **314**, 3684-91.

Kobayashi, T., Liu, X., Wen, F. Q., Kohyama, T., Shen, L., Wang, X. Q., Hashimoto, M., Mao, L., Togo, S., Kawasaki, S. et al. (2006). Smad3 mediates TGF-beta1-induced collagen gel contraction by human lung fibroblasts. *Biochem Biophys Res Commun* **339**, 290-5.

Kohyama, T., Ertl, R. F., Valenti, V., Spurzem, J., Kawamoto, M., Nakamura, Y., Veys, T., Allegra, L., Romberger, D. and Rennard, S. I. (2001). Prostaglandin E(2) inhibits fibroblast chemotaxis. *Am J Physiol Lung Cell Mol Physiol* **281**, L1257-63.

LeClair, R. and Lindner, V. (2007). The role of collagen triple helix repeat containing 1 in injured arteries, collagen expression, and transforming growth factor beta signaling. *Trends Cardiovasc Med* **17**, 202-5.

Li, J., Cao, J., Li, M., Yu, Y., Yang, Y., Xiao, X., Wu, Z., Wang, L., Tu, Y. and Chen, H. (2011). Collagen triple helix repeat containing-1 inhibits transforming growth factor-b1-induced collagen type I expression in keloid. *Br J Dermatol* **164**, 1030-6.

Lin, X., Yu, M., Wu, K., Yuan, H. and Zhong, H. (2009). Effects of pirfenidone on proliferation, migration, and collagen contraction of human Tenon's fibroblasts in vitro. *Invest Ophthalmol Vis Sci* **50**, 3763-70.

Muller, J. M., Metzger, E., Greschik, H., Bosserhoff, A. K., Mercep, L., Buettner, R. and Schule, R. (2002). The transcriptional coactivator FHL2 transmits Rho signals from the cell membrane into the nucleus. *Embo j* **21**, 736-48.

Myllarniemi, M., Lindholm, P., Ryynanen, M. J., Kliment, C. R., Salmenkivi, K., Keski-Oja, J., Kinnula, V. L., Oury, T. D. and Koli, K. (2008). Gremlin-mediated decrease in bone morphogenetic protein signaling promotes pulmonary fibrosis. *Am J Respir Crit Care Med* **177**, 321-9.

Nagai, S., Kitaichi, M., Hamada, K., Nagao, T., Hoshino, Y., Miki, H. and Izumi, T. (1999). Hospital-based historical cohort study of 234 histologically proven Japanese patients with IPF. *Sarcoidosis Vasc Diffuse Lung Dis* **16**, 209-14.

Park, J., Will, C., Martin, B., Gullotti, L., Friedrichs, N., Buettner, R., Schneider, H., Ludwig, S. and Wixler, V. (2008). Deficiency in the LIM-only protein FHL2 impairs assembly of extracellular matrix proteins. *Faseb j* **22**, 2508-20.

Pegorier, S., Campbell, G. A., Kay, A. B. and Lloyd, C. M. (2010). Bone morphogenetic protein (BMP)-4 and BMP-7 regulate differentially transforming growth factor (TGF)-beta1 in normal human lung fibroblasts (NHLF). *Respir Res* **11**, 85.

Pyagay, P., Heroult, M., Wang, Q., Lehnert, W., Belden, J., Liaw, L., Friesel, R. E. and Lindner, V. (2005). Collagen triple helix repeat containing 1, a novel secreted protein in injured and diseased arteries, inhibits collagen expression and promotes cell migration. *Circ Res* **96**, 261-8.

Rubino, C. M., Bhavnani, S. M., Ambrose, P. G., Forrest, A. and Loutit, J. S. (2009). Effect of food and antacids on the pharmacokinetics of pirfenidone in older healthy adults. *Pulm Pharmacol Ther* **22**, 279-85.

Saito, M., Yamazaki, M., Maeda, T., Matsumura, H., Setoguchi, Y. and Tsuboi, R. (2012). Pirfenidone suppresses keloid fibroblast-embedded collagen gel contraction. *Arch Dermatol Res* **304**, 217-22.

Shekhani, M. T., Forde, T. S., Adilbayeva, A., Ramez, M., Myngbay, A., Bexeitov, Y., Lindner, V. and Adarichev, V. A. (2016). Collagen triple helix repeat containing 1 is a new promigratory marker of arthritic pannus. *Arthritis Res Ther* **18**, 171.

Shi, Q., Liu, X., Bai, Y., Cui, C., Li, J., Li, Y., Hu, S. and Wei, Y. (2011). In vitro effects of pirfenidone on cardiac fibroblasts: proliferation, myofibroblast differentiation, migration and cytokine secretion. *PLoS One* **6**, e28134.

Sugiura, H., Liu, X., Kobayashi, T., Togo, S., Ertl, R. F., Kawasaki, S., Kamio, K., Wang, X. Q., Mao, L., Shen, L. et al. (2006). Reactive nitrogen species augment fibroblast-mediated collagen gel contraction, mediator production, and chemotaxis. *Am J Respir Cell Mol Biol* **34**, 592-9.

Sun, Y. W., Zhang, Y. Y., Ke, X. J., Wu, X. J., Chen, Z. F. and Chi, P. (2018). Pirfenidone prevents radiation-induced intestinal fibrosis in rats by inhibiting fibroblast proliferation and differentiation and suppressing the TGF-beta1/Smad/CTGF signaling pathway. *Eur J Pharmacol* **822**, 199-206.

Togo, S., Holz, O., Liu, X., Sugiura, H., Kamio, K., Wang, X., Kawasaki, S., Ahn, Y., Fredriksson, K., Skold, C. M. et al. (2008). Lung fibroblast repair functions in patients with chronic obstructive pulmonary disease are altered by multiple mechanisms. *Am J Respir Crit Care Med* **178**, 248-60.

Upagupta, Shimbori, Alsilmi and Kolb. (2018). Matrix abnormalities in pulmonary fibrosis. *Eur Respir Rev* **27**, 148.

Wixler, V., Hirner, S., Muller, J. M., Gullotti, L., Will, C., Kirfel, J., Gunther, T., Schneider, H., Bosserhoff, A., Schorle, H. et al. (2007). Deficiency in the LIM-only protein Fhl2 impairs skin wound healing. *J Cell Biol* **177**, 163-72.

Wynn. (2008). Cellular and molecular mechanisms of fibrosis. *J Pathol* **214**, 199-210.

Xu, L., Yang, D., Zhu, S., Gu, J., Ding, F., Bian, W., Rong, Z. and Shen, C. (2013). Bleomycin-induced pulmonary fibrosis is attenuated by an antibody against KL-6. *Exp Lung Res* **39**, 241-8.

Yoshida, M., Romberger, D. J., Illig, M. G., Takizawa, H., Sacco, O., Spurzem, J. R., Sisson, J. H., Rennard, S. I. and Beckmann, J. D. (1992). Transforming growth factor-beta stimulates the expression of desmosomal proteins in bronchial epithelial cells. *Am J Respir Cell Mol Biol* **6**, 439-45.

Zhu, Y. K., Liu, X. D., Skold, M. C., Umino, T., Wang, H., Romberger, D. J., Spurzem, J. R., Kohyama, T., Wen, F. Q. and Rennard, S. I. (2001). Cytokine inhibition of fibroblast-induced gel contraction is mediated by PGE(2) and NO acting through separate parallel pathways. *Am J Respir Cell Mol Biol* **25**, 245-53.

611 **Figure legends**

612 **Fig. 1. Effects of pirfenidone on TGF-β1-stimulated collagen gel contraction and**
613 **chemotaxis in HFL-1 cells.** HFL-1 cells were cultured and cast into three-dimensional
614 collagen gels that were maintained in suspension, with gel size measured daily. HFL-1 cells
615 also were grown in a monolayer culture and were trypsinized, and their chemotactic activity
616 towards fibronectin (20 μg/mL) was assessed. (A) Collagen gel contraction on various
617 concentrations of pirfenidone in the presence or absence of 10 pM TGF-β1. (B) Collagen gel
618 contraction following treatment with various concentrations of TGF-β1 in the presence or
619 absence of 100 μg/mL pirfenidone. (C) Number of migrated fibroblasts following treatment
620 with various concentrations of pirfenidone in the presence or absence of 10 pM TGF-β1. (D)
621 Number of migrated fibroblasts following treatment with various concentrations of TGF-β1 in
622 the presence or absence of 100 μg/mL pirfenidone. Collagen gel contraction vertical axis: gel
623 size measured after 2 days of contraction expressed as a percentage of the initial value.
624 Chemotaxis vertical axis: number of migrated cells per five high-power fields (5 HPF).
625 Horizontal axis: conditions. Values represent means ± SEMs of at least three separate
626 experiments. Student's unpaired t test. *$P < 0.05$, **$P < 0.01$, ***$P < 0.001$.

627

628 **Fig. 2. Effects of pirfenidone on collagen gel contraction and chemotaxis in lung**
629 **fibroblasts from controls and patients with interstitial pneumonia (IP).** Fibroblasts from
630 controls and patients with IP were cultured in the presence or absence of pirfenidone (100
631 μg/mL) and 10 pM TGF-β1, and collagen gel contraction and chemotaxis were assayed. (A)
632 Collagen gel contraction. Vertical axis: gel size measured after 2 days of contraction
633 expressed as a percentage of the initial gel area. Horizontal axis: conditions. (B)

Pirfenidone-induced suppression of collagen gel contraction in lung fibroblasts isolated from controls and patients with IP. Vertical axis: percentage of gel contracted size following pirfenidone treatment ([difference of gel size / initial gel size] × 100%). Horizontal axis: conditions. (C) Fibroblast chemotaxis. Vertical axis: number of migrated fibroblasts per 5 HPF. Horizontal axis: conditions. (D) Pirfenidone-dependent suppression of chemotaxis in lung fibroblasts isolated from controls and patients with IP. Vertical axis: percentage of migrated cells following pirfenidone treatment ([difference of migrated cells number / initial migrated cells number] × 100%). Horizontal axis: conditions. Each patient evaluated was expressed as an individual symbol, representing the means of at least two experiments each conducted in triplicate. (A, C) Lines connect the values for individual patients in the presence or absence of pirfenidone. *P < 0.05, **P < 0.01, ***P < 0.001. (B, D) Filled symbols represent UIP, and open symbols represent NSIP. Student's paired t test and unpaired t test. *P < 0.05, **P < 0.01, ***P < 0.001.

Fig. 3. High sensitivity of TGF-β1-induced fibrotic mediators in fibrotic lung fibroblasts. Subconfluent fibroblasts from 12 controls and 12 patients with IP were cultured in serum-free (SF)-DMEM for 24 h and then incubated in the presence or absence of TGF-β1 (10 pM) and/or pirfenidone (100 ng/mL) for 48 h. Proteins from monolayer cultured fibroblasts were extracted and subjected to western blot analysis, and media were harvested from monolayer cultures and evaluated for CTHRC1 and TGF-β1 by immunoassay. Expression of (A) CTHRC1 (30 kDa) and (B) FHL2 (30 kDa) from fibroblasts isolated from controls and patients with IP in the presence or absence of TGF-β1 (10 pM). Vertical axis: expression of proteins normalized to expression of β-actin. Immunoassay of (C) CTHRC1 and (D) TGF-β1. Vertical

axis: mediator production expressed as an amount. Symbols represent the mean values for individual patients, as assessed in two separate experiments. Horizontal axis: conditions. Student's paired t test. *P < 0.05, **P < 0.01.

Fig. 4. Effects of pirfenidone on TGF-β1-mediated fibrotic regulators in lung fibroblasts. Subconfluent HFL-1 cells were cultured in SF-DMEM for 24 h and then incubated in the presence or absence of TGF-β1 (10 pM) and pirfenidone (100 ng/mL) for 48 h. Total protein was extracted, and western blotting was performed with antibodies against the indicated proteins. (A) Western blot analysis of the effects of pirfenidone on targets related to TGF-β1-mediated fibrotic processes, including CTHRC1 (30 kDa), FHL2 (30 kDa), α-SMA (42 kDa), fibronectin (250 kDa), BMP4 (47 kDa), Gremlin1 (25 kDa), and β-actin (42 kDa). The vertical axis shows the relative intensities of (B) CTHRC1, (C) FHL2, (D) α-SMA, (E) fibronectin, (F) BMP4, and (G) Gremlin1 versus β-actin; the horizontal axis shows the conditions. Values represent means ± SEMs of at least three independent experiments. Student's unpaired t test. *P < 0.05, **P < 0.01, ***P < 0.001.

Fig. 5. Effects of pirfenidone on CTHRC1-mediated regulation in lung fibroblasts. Subconfluent HFL-1 cells were cultured in SF-DMEM for 24 h and then incubated in the presence or absence of different concentrations of rhCTHRC1 (see Methods). (A) Western blot analysis of the effects of different concentrations of rhCTHRC1 on targets related to fibrotic processes, i.e., FHL2 (30 kDa), α-SMA (42 kDa), fibronectin (250 kDa), BMP4 (47 kDa), Gremlin1 (25 kDa), and β-actin (42 kDa). Effects of different concentrations of

679 rhCTHRC1 on HFL-1 cell-mediated collagen gel contraction (B) and chemotaxis (C).
680 Subconfluent HFL-1 cells were cultured in SF-DMEM for 24 h and then incubated in the
681 presence or absence of rhCTHRC1 (100 ng/mL) and pirfenidone (100 ng/mL) for 48 h. (D)
682 Western blot analysis of the effects of pirfenidone on rhCTHRC1-mediated targets related to
683 fibrotic processes, i.e., FHL2 (30 kDa), α-SMA (42 kDa), fibronectin (250 kDa), BMP4 (47
684 kDa), Gremlin1 (25 kDa), and β-actin (42 kDa). Effects of pirfenidone on
685 rhCTHRC1-mediated collagen gel contraction (E) and chemotaxis (F). Collagen gel
686 contraction, vertical axis: gel size measured after 2 days of contraction expressed as a
687 percentage of the initial value. Chemotaxis, vertical axis: number of migrated cells per 5 HPF.
688 Horizontal axis: conditions. Effects of pirfenidone on the expression levels of
689 rhCTHRC1-mediated targets assayed using western blot analysis. The vertical axis shows
690 the relative intensities of (G) α-SMA, (H) fibronectin, (I) FHL2, (J) BMP4, (K) Gremlin1 versus
691 β-actin; the horizontal axis shows the conditions. Values represent means ± SEMs of at least
692 three independent experiments. Student's unpaired t test. *$P < 0.05$, **$P < 0.01$, ***$P < 0.001$.
693
694 **Fig. 6. Effects of *CTHRC1* and *FHL2* knockdown in HFL-1 cells.** *CTHRC1*- and
695 *FHL2*-knocked down HFL-1 cells were examined for collagen gel contraction and chemotaxis.
696 (A) Western blot analysis of the effects of *CTHRC1* silencing on targets related to fibrotic
697 processes, i.e., CTHRC1 (30 kDa), FHL2 (30 kDa), α-SMA (42 kDa), fibronectin (250 kDa),
698 BMP4 (47 kDa), Gremlin1 (25 kDa), and β-actin (42 kDa). (B) Collagen gel contraction and
699 (C) chemotaxis after silencing of *CTHRC1*. (D) Western blot analysis of the effects of *FHL2*
700 silencing on targets related to fibrotic processes, i.e., FHL2 (30 kDa), CTHRC1 (30 kDa),
701 α-SMA (42 kDa), fibronectin (250 kDa), BMP4 (47 kDa), Gremlin1 (25 kDa), and β-actin (42

kDa). (E) Collagen gel contraction and (F) chemotaxis after silencing of *FHL2*. Collagen gel contraction, vertical axis: gel size measured after 2 days of contraction expressed as a percentage of the initial value. Chemotaxis, vertical axis: number of migrated cells per 5 HPF. Horizontal axis: conditions. Values represent means ± SEMs of at least three separate experiments. Student's unpaired t test. **P* < 0.05, ***P* < 0.01, ****P* < 0.001.

Fig. 7. Relationship between pirfenidone responses to TGF-β1-stimulated fibroblast bioactivity in vitro and biomarkers of lung fibrosis. Comparison of the relationships between suppression of TGF-β1-induced gel contraction by pirfenidone and serum (A) KL-6 and (B) SP-D levels and between suppression of TGF-β1-induced migration and (C) KL-6 and (D) SP-D levels. Symbols represent individual patients. Linear regression. *P* < 0.05 indicates a positive relationship between pirfenidone response to TGF-β1-stimulated fibroblast bioactivity in vitro and biomarkers of lung fibrosis. (E) Through airway cell/fibroblast interaction, lung fibroblasts are continually exposed to TGF-β1, which is regulated by mediators released by airway cells under inflammatory conditions (Aono et al., 2012) (Xu et al., 2013), resulting in distinct phenotype of fibrotic fibroblasts. This high sensitivity to TGF-β1 along with upregulation of CTHRC1 and FHL2 leads to the development of fibrosis in fibrotic fibroblasts. Treatment with pirfenidone can effectively block this process.

724 **Figures**

725 Fig. 1

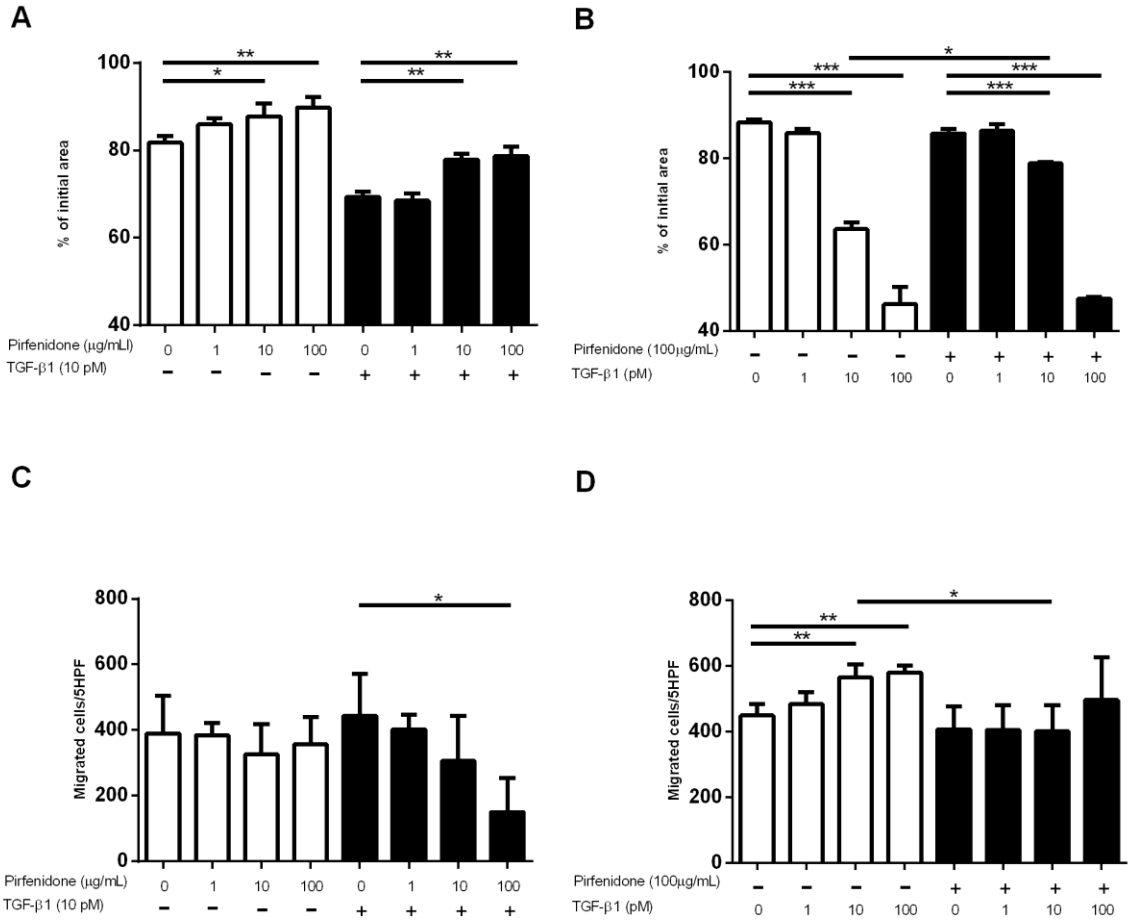

726

727

728

729

730

731

732

733

734

735 Fig. 2

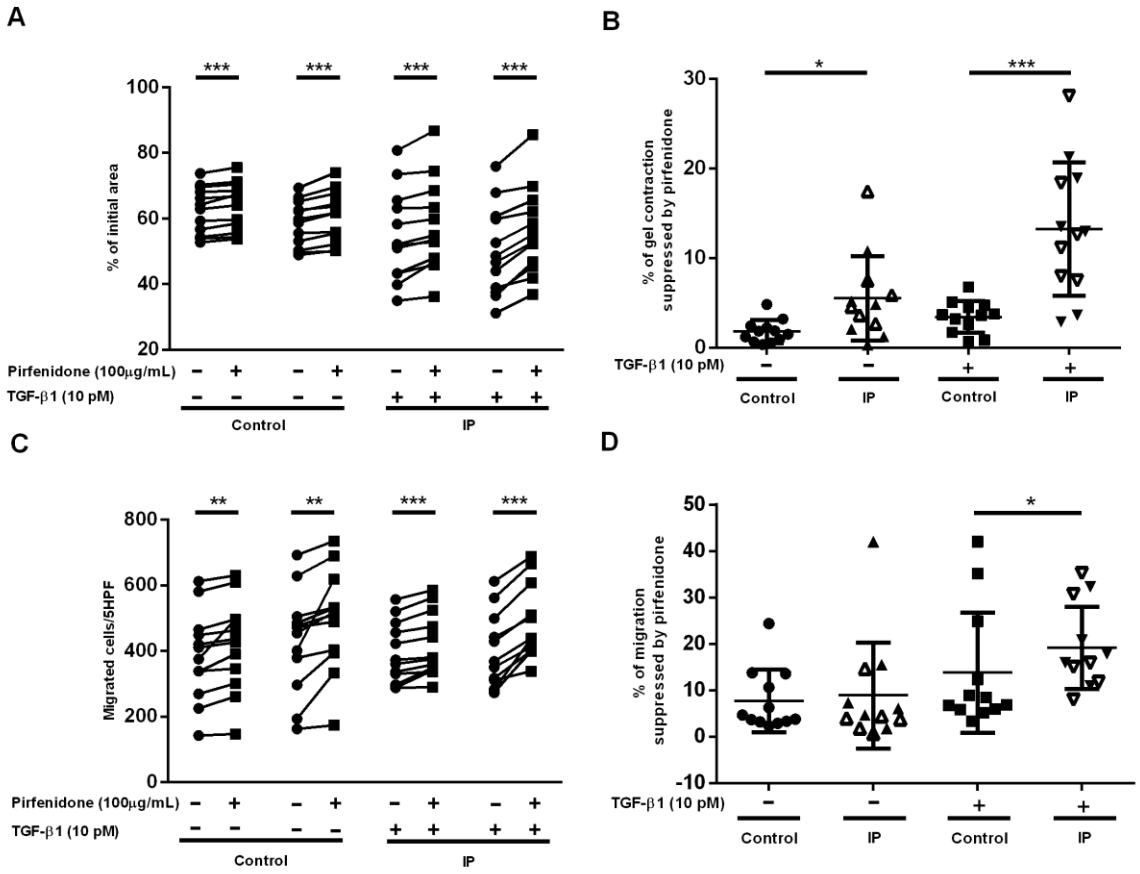

736

737

738

739

740

741

742

743

744

745

746

747 Fig. 3

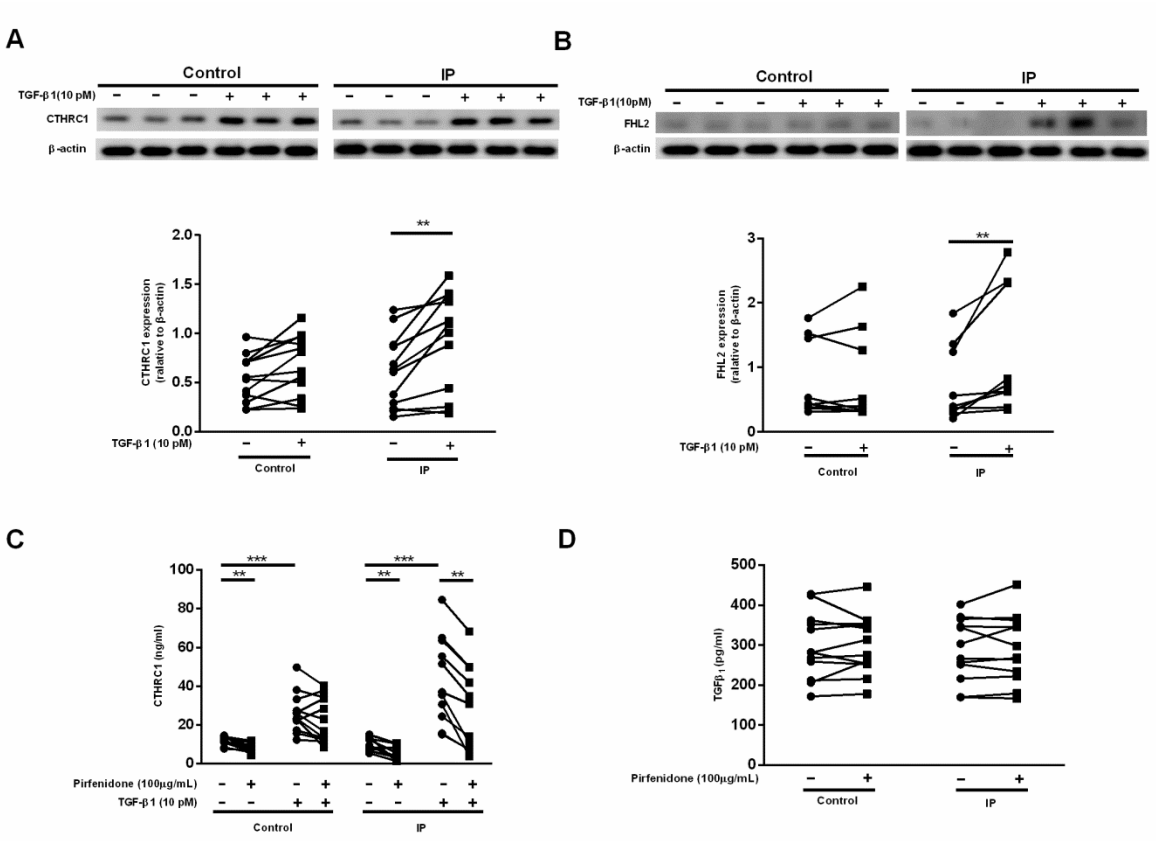

748

749

750

751

752

753

754

755

756

757

758

759

760 Fig. 4

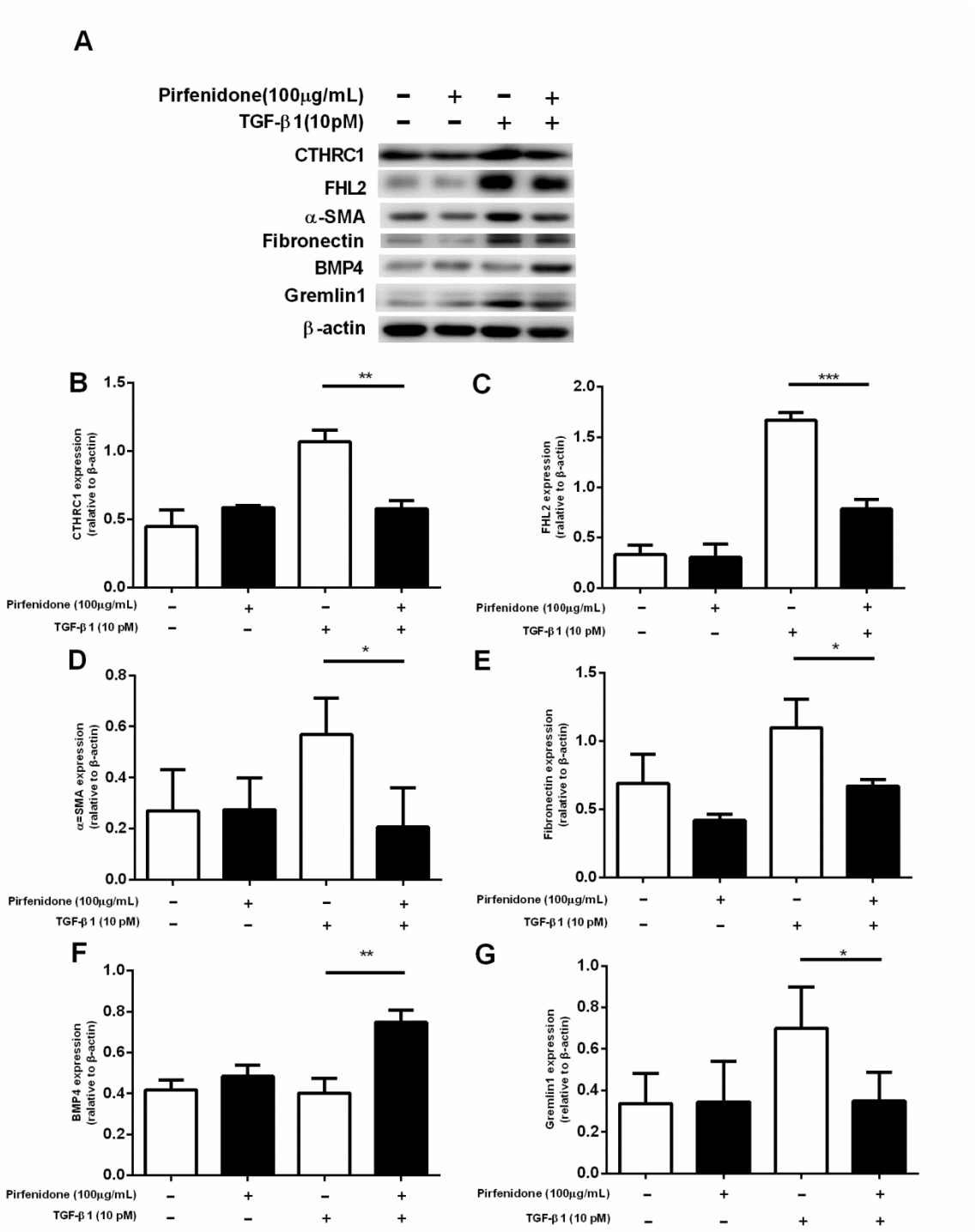

761

762

763

764

765 Fig. 5

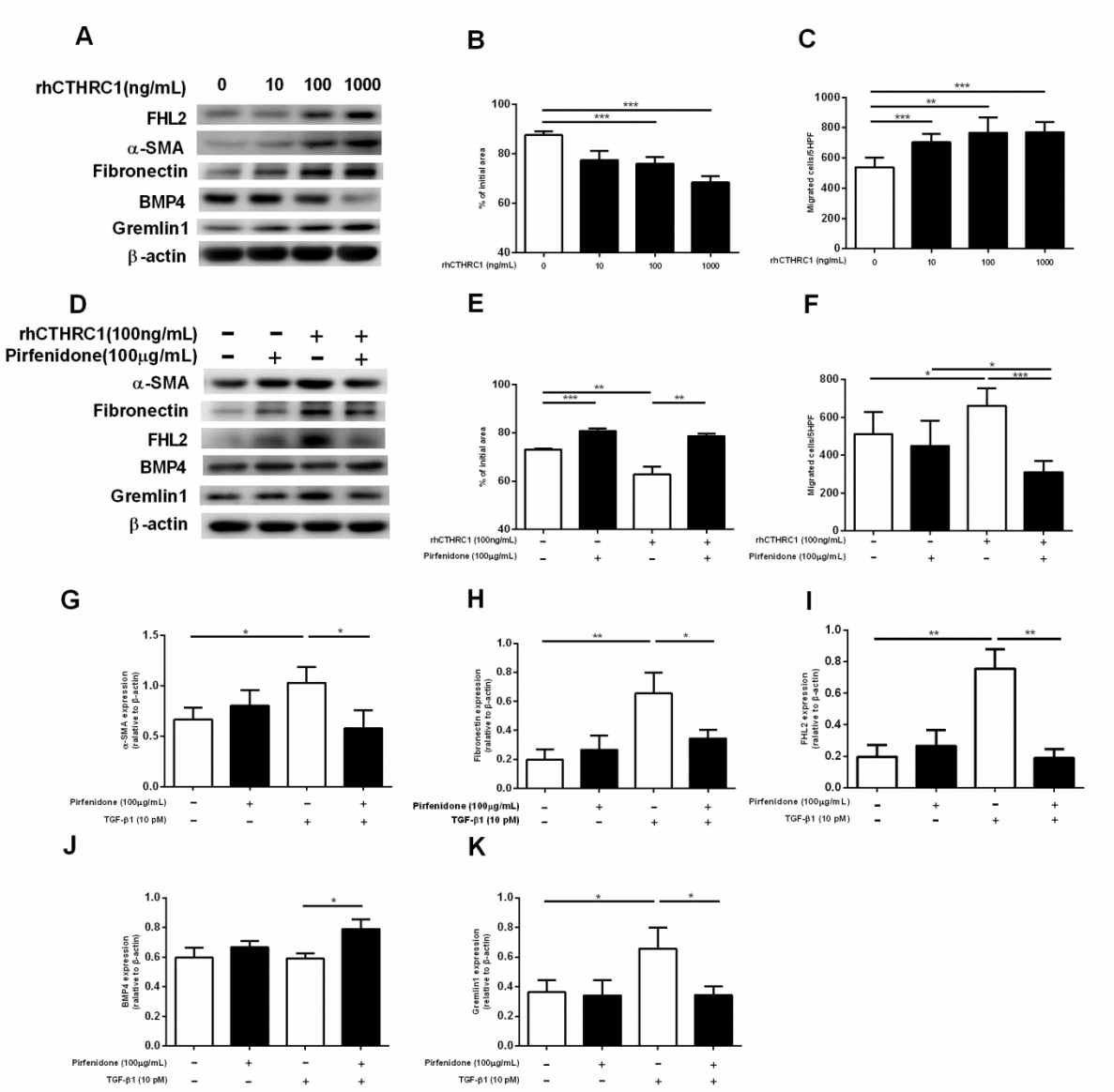

766

767

768

769

770

771

772

773

774 Fig. 6

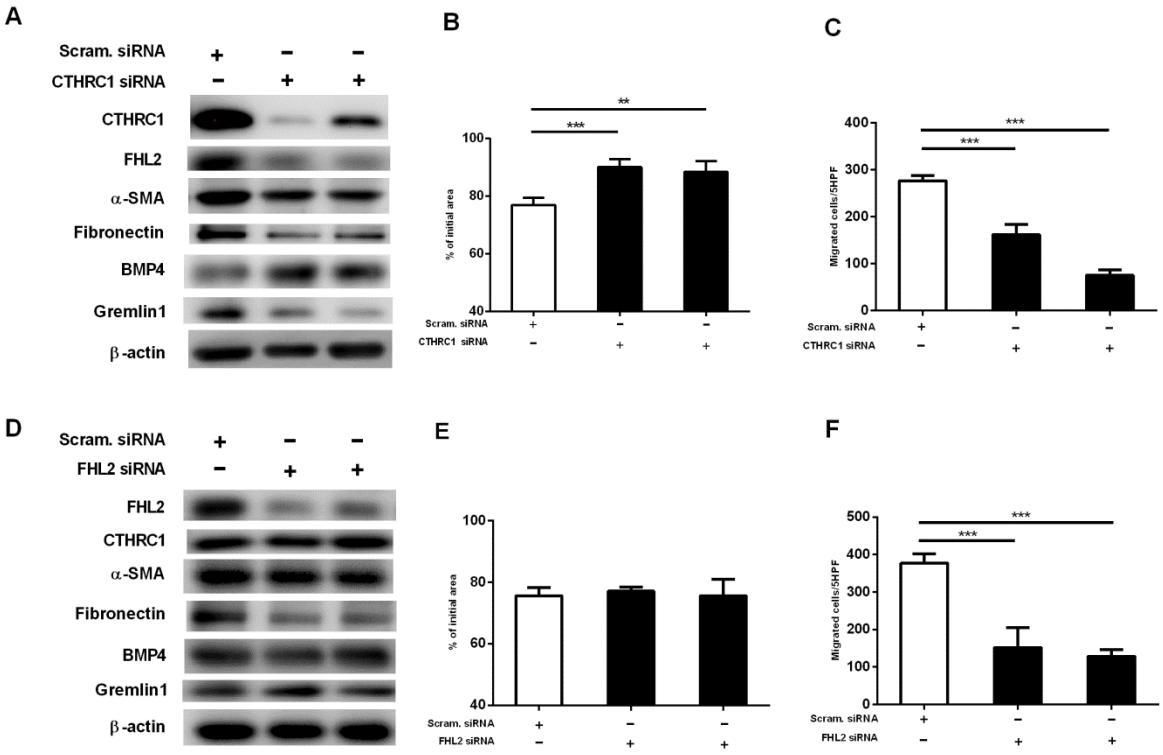

775

776

777

778

779

780

781

782

783

784

785

786

787 Fig. 7

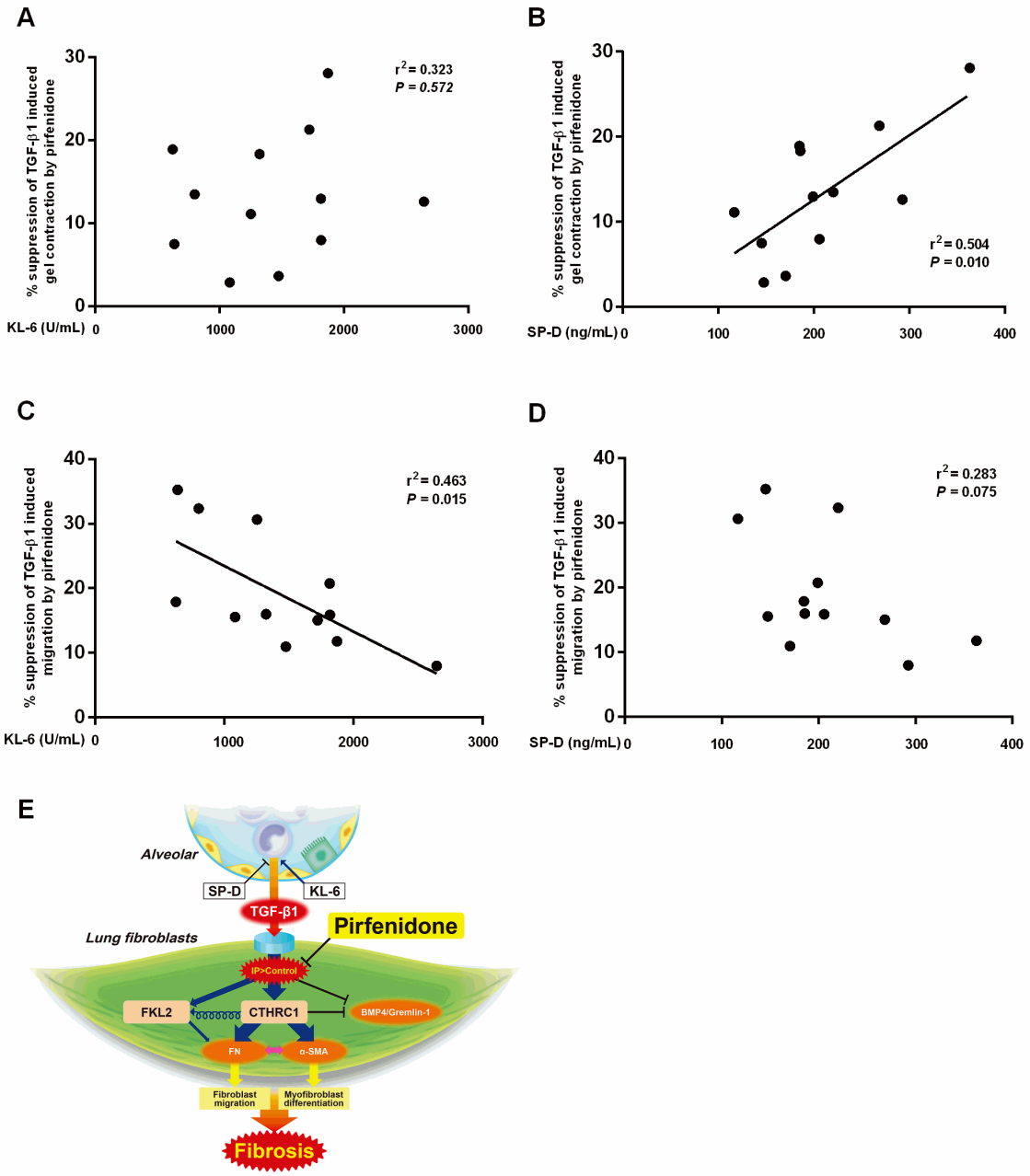

788

789

790

791

792

793

794 **Supplement figure**

795 **Fig. S1. Effects of pirfenidone on TGF-β1-mediated regulators of the cyclooxygenase 2**
796 **(COX2)/prostaglandin E2 (PGE2) pathway in fibroblasts.** Subconfluent HFL-1 cells were
797 cultured in SF-DMEM for 24 h and then incubated in the presence or absence of TGF-β1 (10
798 pM) and pirfenidone (100 ng/mL) for 48 h. Proteins were extracted and subjected to western
799 blot analysis of COX2. Media were harvested from monolayer culture and evaluated for
800 PGE2 by immunoassay. (A) Release of PGE2 in HFL-1 monolayer cultures and (B) western
801 blot analysis of COX2 (69 kDa). Bar figure vertical axis: protein expression relative to β-actin.
802 Horizontal axis: conditions. Values represent means ± SEMs of at least three independent
803 experiments.
804
805
806
807
808
809
810
811
812
813
814
815
816

817 **Fig. S1.**

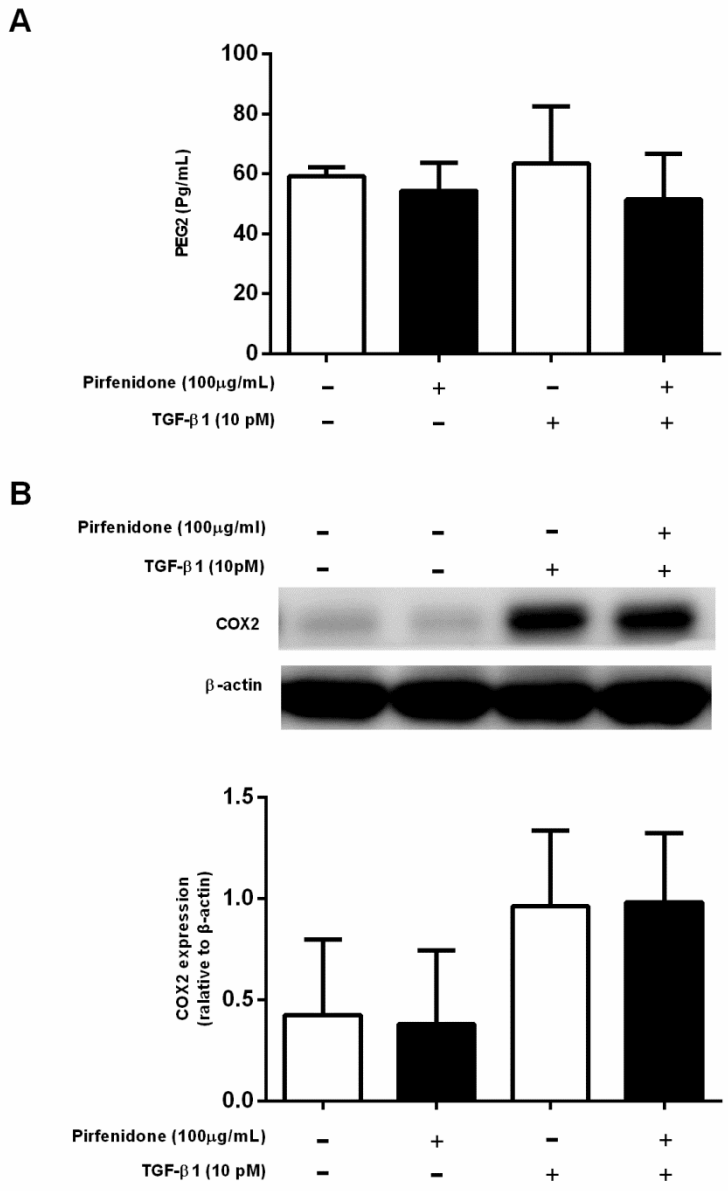

818